Analysis of Intact Monoclonal Antibody IgG1 by Electron Transfer Dissociation Orbitrap FTMS*[S]

Luca Fornelli‡, Eugen Damoc§, Paul M. Thomas¶, Neil L. Kelleher¶, Konstantin Aizikov§, Eduard Denisov§, Alexander Makarov§, and Yury O. Tsybin‡‖

The primary structural information of proteins employed as biotherapeutics is essential if one wishes to understand their structure–function relationship, as well as in the rational design of new therapeutics and for quality control. Given both the large size (around 150 kDa) and the structural complexity of intact immunoglobulin G (IgG), which includes a variable number of disulfide bridges, its extensive fragmentation and subsequent sequence determination by means of tandem mass spectrometry (MS) are challenging. Here, we applied electron transfer dissociation (ETD), implemented on a hybrid Orbitrap Fourier transform mass spectrometer (FTMS), to analyze a commercial recombinant IgG in a liquid chromatography (LC)-tandem mass spectrometry (MS/MS) top-down experiment. The lack of sensitivity typically observed during the top-down MS of large proteins was addressed by averaging time-domain transients recorded in different LC-MS/MS experiments before performing Fourier transform signal processing. The results demonstrate that an improved signal-to-noise ratio, along with the higher resolution and mass accuracy provided by Orbitrap FTMS (relative to previous applications of top-down ETD-based proteomics on IgG), is essential for comprehensive analysis. Specifically, ETD on Orbitrap FTMS produced about 33% sequence coverage of an intact IgG, signifying an almost 2-fold increase in IgG sequence coverage relative to prior ETD-based analysis of intact monoclonal antibodies of a similar subclass. These results suggest the potential application of the developed methodology to other classes of large proteins and biomolecules. ***Molecular & Cellular Proteomics 11: 10.1074/mcp.M112.019620, 1758–1767, 2012.***

Top-down mass spectrometry (MS)[1] (1–3) has continued to demonstrate its particular advantages over traditionally employed bottom-up MS strategies (4). Specifically, top-down MS allows the characterization of specific protein isoforms originating from the alternative splicing of mRNA that code single nucleotide polymorphisms and/or post-translational modifications (PTMs) of protein species (5). Intact protein molecular weight (MW) determination and subsequent gas-phase fragmentation of selected multiply charged protein ions (referred to as tandem MS or MS/MS) theoretically might result in complete protein sequence coverage and precise assignment of the type and position of PTMs, amino acid substitutions, and C- or N-terminal truncations (6), whereas the bottom-up MS approach allows only the identification of a certain protein family when few or redundant peptides are found for a particular protein isoform. At a practical level, however, top-down MS-based proteomics struggles not only with the single- or multi-dimensional separation of undigested proteins, which demonstrates lower reproducibility and repeatability than for peptides, but also with technical limitations present in even state-of-the-art mass spectrometers. The outcome of a top-down MS experiment depends indeed on the balance between the applied resolution of the mass spectrometer and its sensitivity. The former is required for unambiguous assignment of ion isotopic clusters in both survey and MS/MS scans, whereas the latter is ultimately dependent on the scan speed of the mass analyzer, which determines the number of scans that can be accumulated for a given analyte ion on the liquid chromatography (LC) timescale to enhance the resulting signal-to-noise ratio (SNR). Until recently, the instrument of choice for top-down MS has been the Fourier transform ion cyclotron resonance (FT-ICR) mass

From the ‡Biomolecular Mass Spectrometry Laboratory, Ecole Polytechnique Fédérale de Lausanne, 1015 Lausanne, Switzerland; §Thermo Fisher Scientific (Bremen) GmbH, Hanna-Kunath Str. 11, 28199 Bremen, Germany; ¶Departments of Chemistry and Molecular Biosciences and the Proteomics Center of Excellence, Northwestern University, Evanston, Illinois 60208

Received April 13, 2012, and in revised form, August 18, 2012
Published, MCP Papers in Press, September 10, 2012, DOI 10.1074/mcp.M112.019620

[1] The abbreviations used are: ETD, electron transfer dissociation; ECD, electron capture dissociation; CID, collision-induced dissociation; FT, Fourier transform; FTMS, Fourier transform mass spectrometry; IgG, immunoglobulin G; MS, mass spectrometry; MS/MS, tandem mass spectrometry; LC, liquid chromatography; PTM, post-translational modification; SNR, signal-to-noise ratio; FT-ICR MS, Fourier transform ion cyclotron resonance mass spectrometry; MW, molecular weight; qTOF MS, quadrupole time-of-flight mass spectrometry; LTQ, linear trap quadrupole (linear ion trap); pyroGlu, pyroglutamic acid.

spectrometer, primarily because of its superior resolving power and the availability of electron capture dissociation for the efficient MS/MS of large biomolecules (7, 8). However, this solution has been shown to have some limitations in the analysis of large proteins (9). The main issue, as described by Compton *et al.* (10), is that the SNR in Fourier transform mass spectrometry (FTMS) is inversely proportional to the width of the isotopic and charge state distributions (11), which both increase as a function of MW. Particularly, the SNR dramatically decreases with MW under standard on-line LC-MS/MS operating conditions if isotopic resolution is required. It is noteworthy that such SNR reduction can affect not only intact mass measurements, but also the subsequent MS/MS performance.

The most widely employed solution for improving top-down analysis is thus a substantial reduction of the protein mixture complexity, for example, through off-line sample prefractionation (12). Furthermore, when the MW exceeds 100 kDa, proteins are often analyzed *via* direct infusion after off-line purification of the single isoform or species of interest (13). Overall, these strategies aim to improve the quality of mass spectra, specifically their SNR, by increasing the number of scans dedicated to each selected isoform or species. However, off-line intact protein analysis has limitations, including sample degradation and modification (*e.g.*, oxidation during long off-line measurements and sample storage). The time required for multistep LC-based protein purification can also be substantial.

Electron capture dissociation (ECD) (14, 15) and electron transfer dissociation (ETD) (16) are ion activation techniques that allow polypeptide fragmentation with reduced PTM losses (17, 18). Nevertheless, ECD and ETD generally provide larger sequence coverage for intact proteins than slow-heating activation methods such as collision induced dissociation (CID) and infrared multiple photon dissociation (19, 20). Furthermore, ECD and ETD are known to cleave disulfide bonds, a fundamental feature for the analysis of proteins in their native state (*i.e.*, without cysteine reduction and alkylation) (21–23).

The structural analysis of high MW intact proteins with MS has garnered much recent attention in the literature (24, 25), mainly because of the improved capabilities offered by rapidly developing sample preparation, protein separation, and mass spectrometric methods and techniques. Immunoglobulin G (IgG) proteins are antibodies with an MW of about 150 kDa that are composed of two identical sets of light and glycosylated heavy chains with both intra- and intermolecular disulfide bridges (Fig. 1) (26). IgGs represent an attractive target for structural analysis method development, given their high importance as biotherapeutics (27). A unit-mass resolution mass spectrum demonstrating an isotopic distribution of an isolated charge state of a 148 kDa IgG1 has been recently achieved with FT-ICR MS equipped with 9.4 T superconducting magnet and a statically harmonized ICR cell (24). However, further

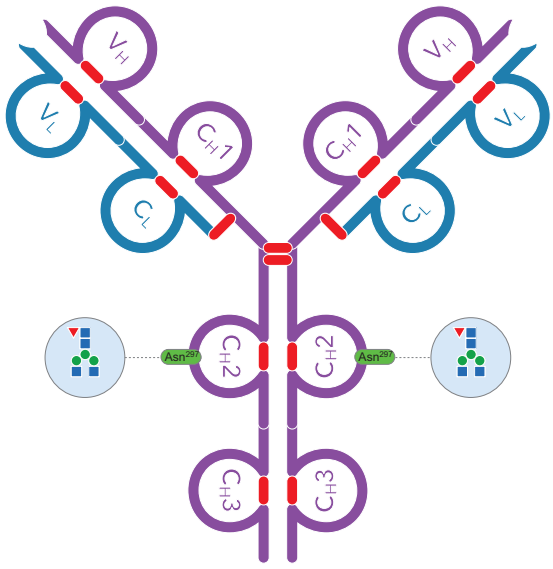

FIG. 1. **Schematic representation of IgG1.** Two identical light (*blue*) and two identical heavy (*fucsia*) chains form the intact IgG. The light chain is composed of a variable domain (V_L) and a constant domain (C_L), whereas the heavy chain comprises one variable domain (V_H) and three constant domains (C_H1–3). Each domain contains an intramolecular disulfide bridge (in *red*); intermolecular disulfide bridges link the heavy chains to each other (two bonds) and each heavy chain to one light chain (one bond). Each heavy chain includes an N-glycosylation site (located at Asn^{297}; here, a G0F/G0F glycosylation is shown).

analytical improvements are needed to achieve routine and reproducible MS operation at the required level of resolution and sensitivity.

Fragmentation of intact antibodies in the gas phase following the top-down MS approach has been previously attempted without precursor ion charge state isolation by means of nozzle-skimmer CID on a linear trap quadrupole (LTQ)-Orbitrap™ (28, 29) and with precursor ion isolation *via* ETD on a high resolution quadrupole time-of-flight (qTOF) mass spectrometer (25). Relative to the results previously obtained with slow-heating MS/MS methods, the ETD qTOF MS/MS demonstrated substantially higher sequence coverage, reaching 15% for human and 21% for murine IgGs. Important for future top-down proteomics development for complex protein mixtures, the ETD qTOF MS/MS results were obtained on the LC timescale. To increase the sequence coverage and confidence in product ion assignment, a substantial increase in SNR was achieved by averaging MS/MS data from up to 10 identical LC-MS/MS experiments. The high complexity of the product ion population reduced the effective resolution to about 30,000, presumably limiting the assignment of overlapping high charge state product ions in the 1000–2000 *m/z* range. Even higher peak complexity was observed in the region of charge reduced species and complementary heavy product ions, above 3000 *m/z*. Finally, numerous disulfide bonds drastically reduced MS/MS efficiency in the disulfide bond-protected regions.

Here we demonstrate that ETD-enabled hybrid linear ion trap Orbitrap FTMS allows us to further improve the top-down ETD-based LC-MS/MS of monoclonal antibodies, introduced earlier for TOF-based MS. To fully take advantage of the high resolving power of Orbitrap MS/MS for increasing both the number of assigned product ions and the confidence of the assignments, maintaining an LC-MS/MS setup useful in a general proteomics workflow for protein desalting and separation, we averaged time-domain transients (derived from separated LC-MS/MS runs) before Fourier transform signal processing.

EXPERIMENTAL PROCEDURES

Sample Preparation—Humira monoclonal IgG1, *kappa*, was kindly provided by Abbott Laboratories (Abbott Park, IL, USA). The protein, originally stored in a buffer solution (sodium phosphate/sodium citrate/polysorbate 80, with the addition of NaCl), was dissolved in water at a concentration of 10 μM and used without further purification.

Liquid Chromatography—Protein desalting and preconcentration for subsequent on-line MS/MS analysis was performed with reverse phase high performance LC (Surveyor MS Pump Plus with Micro Autosampler, Thermo Fisher Scientific, San Jose, CA, USA). For each chromatographic run, 20 pmol (2 uL) of IgG was loaded onto a BioBasic-4 column of 1 mm i.d. and 100 mm length with a 5 μm particle size (Thermo Fisher Scientific, Runkorn, UK). A linear gradient from 20% to 80% of acetonitrile with 0.1% formic acid at a 100 μl/min flow rate was applied to ensure an IgG elution time of ~5 min. The total run time, including column wash and re-equilibration, was about 15 min.

MS and Tandem MS—An ETD-enabled hybrid linear ion trap Orbitrap FTMS (Orbitrap Velos Pro, Thermo Scientific, Bremen, Germany) with an IonMAX ion source was employed for both IgG intact mass measurement and fragmentation, in separate experiments. For ETD MS/MS, precursor ions were isolated at either 2750 ± 50 *m/z* (hereinafter referred to as the "narrow isolation window") or 2900 ± 300 *m/z* (hereinafter referred to as the "wide isolation window") in the high pressure LTQ. Fluoranthene radical anions were introduced into the LTQ over 40 to 50 ms and were allowed to interact with multiply charged cations of IgG for 10 or 25 ms. Product ions were transferred to the Orbitrap FTMS, which was operated with a charge target value (automatic gain control) set to 1 million. Precursor and product ion detection were performed in the Orbitrap mass analyzer over a 200–4000 *m/z* range. The resolving power was set at 15,000 (at 400 *m/z*) for MS experiments and at 100,000 (at 400 *m/z*) for ETD MS/MS. The precursor ion target was set to 1×10^6 for all experiments, and the target for fluoranthene anions was set to 2×10^6. To optimize the SNR improvement as a function of single scan number, 10 microscans were averaged for each scan in all the experiments. The S-lens rf level was set to the maximum (70), and the transfer tube temperature was set to 350 °C. Sheath gas was set to 20, and auxiliary to 10. The Orbitrap FTMS was calibrated for the high (2000–4000 *m/z*) mass range, keeping mass accuracy for the low (50–2000 *m/z*) mass range at the acceptable level.

Tandem MS Data Processing and Analysis—For each ETD LC-MS/MS experiment, Orbitrap FTMS time-domain transients were recorded in MIDAS .dat format (30) for additional signal processing. A dedicated routine was developed in-house for recording and adding the transients. Briefly, transient recording can be performed either directly by the Orbitrap FTMS on-board computer or through an additional oscilloscope connected to the preamplifier outputs, as described elsewhere (31). Transient processing was performed following standard methods developed for FT-ICR MS, taking advantage of the Orbitrap FTMS transient MIDAS format's being fully compatible with the available FT-ICR MS data analysis freeware (32). Importantly, all transient signals originating from separate LC-MS/MS experiments were summed in the time domain prior to Fourier transform (FT) signal processing. In the current work, the following numbers of summed transients were realized: (i) 18 scans (corresponding to 180 microscans) from a single LC-MS/MS run with an ETD duration of 10 or 25 ms; (ii) 180 scans (1800 microscans) from 10 LC-MS/MS runs with either 10 or 25 ms ETD; (iii) 360 scans (3600 microscans) from 20 LC-MS/MS runs, with equal numbers of 10 and 25 ms ETD experiments; and (iv) 1000 scans (10,000 microscans) from 40 LC-MS/MS runs, with 10 and 25 ms ETD combined.

For the SNR estimation, the noise in the ETD mass spectra was first calculated point by point (in a 45 *m/z* unit-large portion of the mass spectra, always the same for all of the ones considered), and after that the abundance of the peak at 772 *m/z* (taken as a reference for the light product ion population) was divided over the obtained noise value. Mass spectral deconvolution was performed with ProMass software (Thermo Scientific), and comprehensive analysis of fragmentation patterns was performed with the dedicated top-down MS analysis software ProSight PC 2.0 (Thermo Scientific) (33). In the ProSightPC analysis, searches were performed against a custom protein warehouse incorporating the known sequences of both light and heavy chains of Humira in both oxidized and reduced forms (both chains) and with both cyclized and uncyclized isoforms of the heavy chain. Data were searched in two ways: first at ±15 ppm fragment tolerance, and finally at ±4.2 Da fragment tolerance. Fragments matching the first search were considered valid without further inspection. Data acquired in the second search were all manually validated. The large search tolerance required for these analyses arises from two separate phenomena: first, peak picking algorithms can mismatch the isotopic distribution, and second, electron-based fragmentations are known to undergo hydrogen atom migration (34, 35). Both of these processes can shift the observed mass by 1 or more Da (1.0033 Da in the former, 1.0078 Da in the latter). Spurious matches were removed as false positives in this analysis.

RESULTS

Intact Protein MS—Fig. 2 shows the results of a single LC-MS experiment, without fragmentation, on the human, recombinant Humira IgG1. Over the selected gradient, the elution time of the IgG from the column was ~5 min (Fig. 2*A*). The gradient, in combination with the relatively high quantity of IgG injected, maximized the elution time and allowed for efficient desalting. The charge state distribution is centered on the 52+ protein cation, and charge states observed ranged from 38+ to 80+ (Fig. 2*B*). After the deconvolution of broadband MS data, several potential glycoforms were identified (Fig. 2*C*). The peak at 148,080.3 Da can be attributed to two G0F oligosaccharidic chains (often referred to as G0F/G0F glycoform (36)), whereas the remaining two glycoforms can be considered, respectively, as a G0F/G1F glycoform (considered the mass difference of 162 Da, corresponding to the addition of a hexose to one of the oligosaccharides) and G1F/G1F (or possibly, but less likely, G0F/G2F). Considering the known sequence of the IgG, which corresponds to an average mass of 145,465.5 Da, the mass accuracy error for the first glycan combination is ~0.3 Da, corresponding to ~2 ppm. The wide charge state envelope (from 38 to 80+) ensured good statistics for the deconvolution operation. The

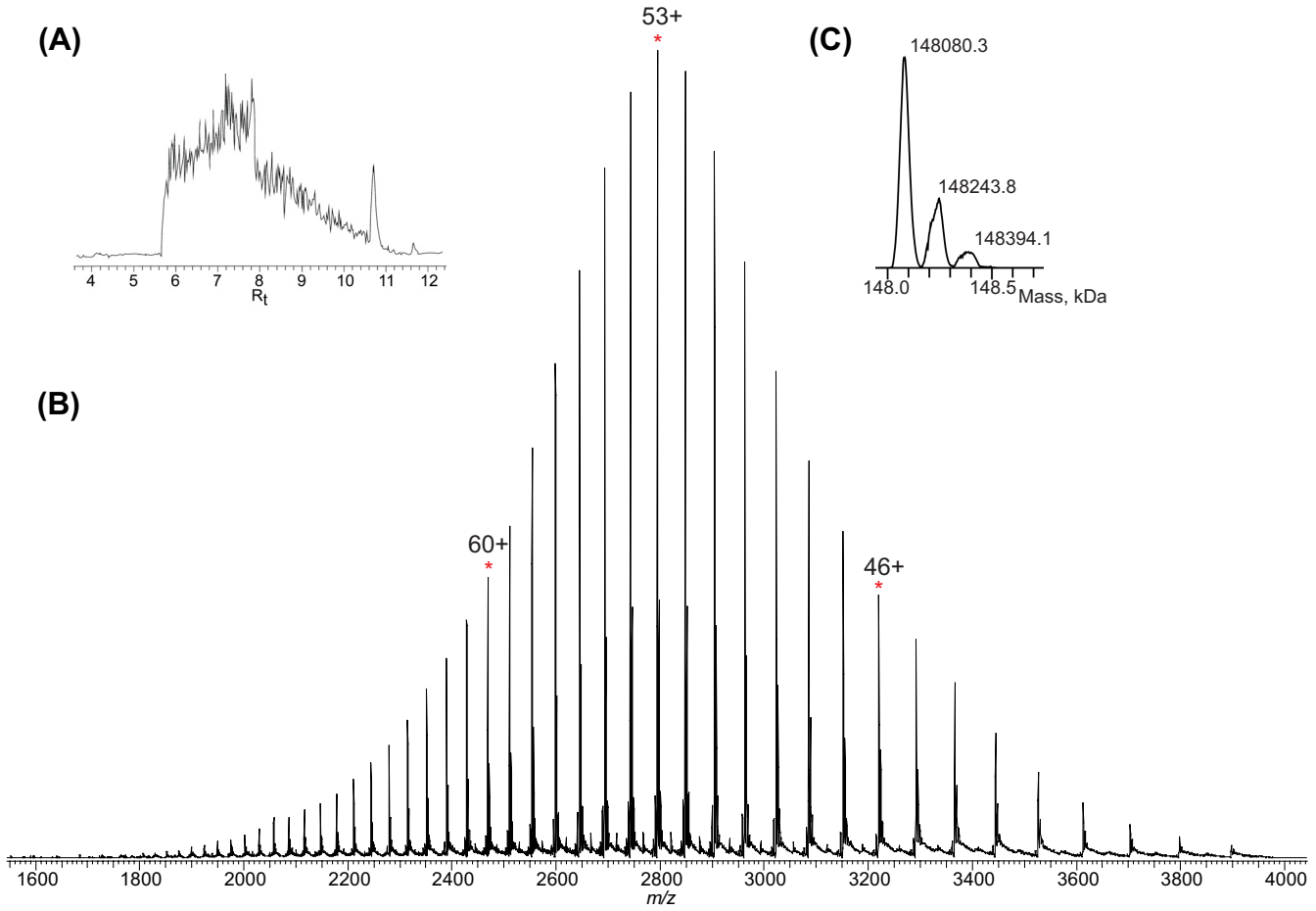

FIG. 2. **Results of intact IgG LC-MS analysis in the Orbitrap FTMS acquired at 15,000 resolution (at *m/z* 400).** *A*, base peak chromatogram displaying the ~5 min elution of the analyzed IgG1. *B*, charge state distribution of the Humira IgG, from 38+ to 80+. *C*, Deconvoluted mass spectrum showing distinct IgG glycoforms; the first peak represents a G0F/G0F glycoform, and the second and third peaks are G0F/G1F and G1F/G1F, respectively.

inferred glycosylation pattern for the Humira IgG1 produced by intact protein mass measurements is consistent with what reported in the literature for similarly produced antibodies (36, 37). Moreover, the intact mass measurements confirmed that no truncation was observed at either the N- or the C-terminus of the analyte.

Typically, qualitative and quantitative analysis of the glycosylation profile are performed in a bottom-up fashion—for instance, by quantifying tryptic glycopeptides (38). However, and more commonly, in order to reduce the high complexity of all possible combinations of different glycans that can be found on recombinant IgGs, glycans are released *via* enzymatic reaction with PNGase F (39), with or without combination with physical methods such as microwave-assisted digestion (40), for both qualitative and quantitative analysis.

Top-down MS Method Optimization—As previously mentioned, the main performance limitation in the LC-based top-down MS and MS/MS of large proteins is the relatively low SNR provided by averaging a limited number of scans acquired during rapid protein elution in a single LC-MS/MS experiment. To increase the SNR of the MS/MS data and to maximize the number of confidently identified product ions, summing of Orbitrap MS/MS transients coming from a number of distinct LC-MS/MS experiments could be implemented before performing FT for time-to-frequency conversion. Fig. 3 displays expanded segments of ETD mass spectra resulting from analysis of a different numbers of transients acquired for two ion–ion interaction periods (10 ms and 25 ms) and two isolation windows (narrow and wide). Figs. 3*A*–3*E* show the results of experiments performed with a 2700–2800 *m/z* precursor ion isolation window in the LTQ, the narrow isolation window, comprising precursor ions from 53+ to 55+ charge states. The ETD mass spectrum shown in Fig. 3*F* was obtained for the 2600–3200 *m/z* precursor ion isolation window, the wide isolation window, comprising precursor ions from 47+ to 57+ charge states. For a 10 ms ion–ion interaction period (ETD duration), the main product ion population is centered at about 1600 *m/z*, and a second group of less abundant, lighter product ions is located below 1000 *m/z* (Fig. 3*A*). The experiment with a longer (25 ms) ETD duration shows

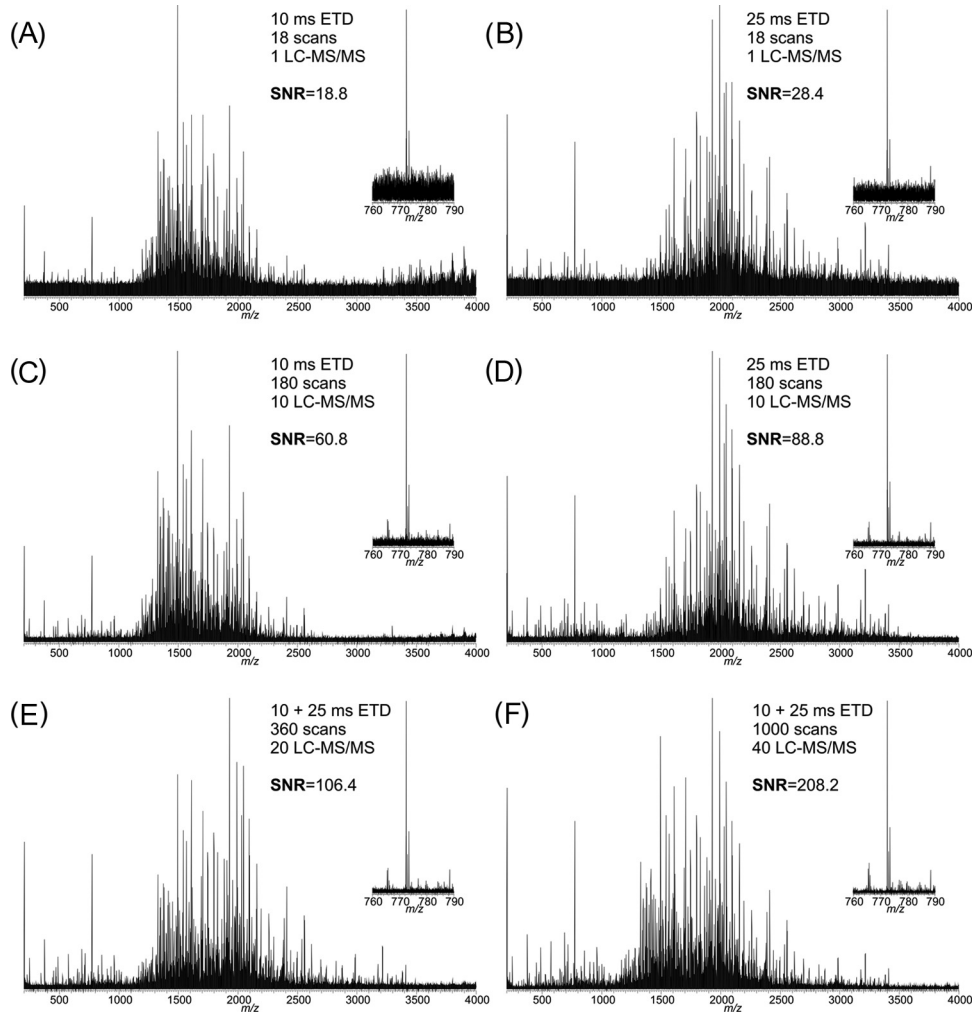

FIG. 3. **Comparison of ETD mass spectra resulting from the addition of different numbers of transients and acquired under different ETD conditions.** Precursor ion isolation window for panels *A–E* was 2750 ± 50 *m/z*, whereas for panel *F* a wider isolation window of 600 *m/z* units centered at 2900 *m/z* was employed. *A*, ETD mass spectra obtained by summing 18 scans (corresponding to 180 microscans) acquired in a typical single ETD LC-MS/MS experiment with 10 ms ETD duration. *B*, single LC-MS/MS with 25 ms ETD duration. *C*, ETD mass spectra obtained by summing 180 transients (corresponding to 1800 microscans) collected in 10 LC-MS/MS experiments with 10 ms ETD duration. *D*, 10 LC-MS/MS runs with 25 ms ETD duration. *E*, ETD mass spectrum resulting from the sum of 360 transients, coming equally from 10 ms and 25 ms ETD duration experiments, equivalent to 20 LC-MS/MS runs. *F*, ETD mass spectrum resulting from the sum of 1000 transients (10,000 microscans in total), coming equally from 10 ms and 25 ms ETD duration experiments.

a clear mass shift toward higher *m/z* values, with the final result being that the main product ion population is centered at ~2000 *m/z* (Fig. 3*B*). A longer ETD duration presumably causes secondary electron transfer and product ion fragmentation. A greater number of different product ions with low masses is present in Fig. 3*B* than in Fig. 3*A*. Under both experimental conditions, the precursor ions and the corresponding charge-reduced species were barely detectable. This contrasts with our previous ETD MS/MS analysis of a human IgG conducted on a qTOF MS (for a comparison, see Fig. 1 of Ref. (25)). Figs. 3*C* and 3*D* show ETD mass spectra obtained by summing 180 scans from 10 and 25 ms ETD LC-MS/MS experiments, respectively. Here, the lack of detected IgG charge-reduced species is even more apparent. Finally, Figs. 3*E* and 3*F* display mass spectra combining scans from both 10 and 25 ms ETD MS/MS, with the former resulting from the sum of 360 scans and the latter 1000 scans coming from ETD experiments in which a wide isolation window was used. These two ETD mass spectra present a bimodal product ion distribution character. Note that in addition to the increase in SNR for mass spectra gained by summing experiments with ETD interaction times of 10 ms and 25 ms, it is believed that higher sequence coverage may be obtained by adding potentially different product ions produced at a different degree of secondary fragmentation.

To estimate the sensitivity (or SNR) gain achieved by summing time domain transients before FT, we calculated SNR values for each of the ETD mass spectra presented in Fig. 3

using the abundance of the 772 *m/z* ion peak as a reference (see insets in Fig. 3). The reference peak was selected for its presence in both the 10 ms and 25 ms ETD experiments and its location in a spectral region with low interference from other peaks. Although the abundance of the 772 *m/z* ion peak relative to that of the base peak changes between the 10 ms and 25 ms datasets, it is clear that the measured SNR is roughly tripled when the number of scans increases from 18 to 180, as expected (the SNR goes from 18.8 to 60.8 and from 28.4 to 88.8 in 10 ms and 25 ms experiments, respectively). For ETD mass spectra combining an equal number of scans from the two types of ETD experiments, the gain in SNR is more difficult to determine, but by considering an averaged value for the initial SNR at 18 scans (that is, (18.8 + 28.4)/2 = 23.6) we can assume an increment of more than 4 times for the ETD mass spectrum in Fig. 3*E* relative to the result of a single LC-MS/MS experiment. The same calculation returns an almost 9-fold increment for the 1000-scans averaged ETD mass spectrum, which results from the use of different ETD precursor ions due to a wider isolation window and thus is not fully comparable with the preceding examples. A further increase in SNR obtained by adding more LC-MS/MS runs is feasible, although the envisioned SNR gain might not be justified by the increased sample consumption and experiment duration. Therefore, other ways of improving SNR in a single LC-MS/MS experiment are to be explored, including (i) activated ion-ETD (35, 41), (ii) protein ion supercharging (42–45), (iii) an increased number of precursor ions obtained through multiple fills of the ETD reaction cell, (iv) improved product ion transmission to the Orbitrap mass analyzer from the ETD reaction cell, and (v) an increased number of scans acquired per LC-MS/MS experiment *via* super-resolution-method-based signal processing applied complementary to the FT signal processing (46).

The complexity of high SNR ETD mass spectra can be appreciated in Fig. 4, which emphasizes the importance of the employed high resolution acquisition (100,000 at 400 *m/z*) in the MS/MS mode. Particularly, the overlapping isotopic distributions of multiply charged product ion clusters are resolved, allowing one to determine their charge state with high confidence. Although the high resolution employed in this work profoundly contributed to the identification of IgG backbone cleavage sites (*vide infra*), it must be stressed that the increase in SNR achieved with the addition of transients taken from different LC-MS/MS experiments (see supplemental Fig. S1) is currently the most important factor for the successful analysis of populations of large, multiply charged product ions *via* FTMS.

ETD-based Top-down MS: Narrow Isolation Window—The mass spectra obtained by summing 360 and 1000 ETD MS/MS scans were subjected to data analysis with ProSight PC (see "Experimental" section for more details). The obtained fragmentation map is represented in Fig. 5. A summary of identified N- and C-terminal end-containing ions for both

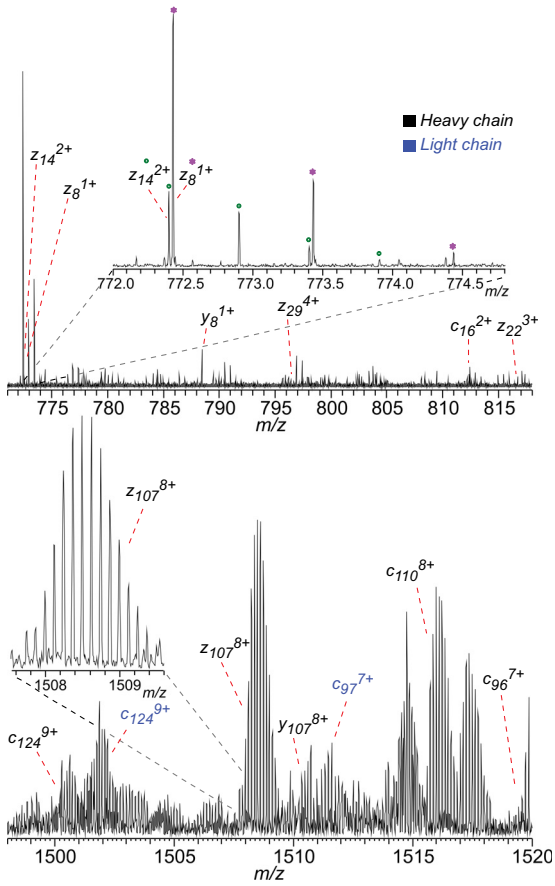

FIG. 4. **Expanded segments of ETD mass spectrum obtained by averaging 1000 scans (mass spectrum shown in Fig. 3*F*).** *Upper panel*, low *m/z* region; the importance of the high resolution in discriminating between z_{14}^{2+} and z_8^{1+} (heavy chain) is confirmed in the inset. *Bottom panel*, expanded segment of an ETD mass spectrum with highly charged and partially overlapping product ion clusters; the isotopic distribution of z_{107}^{8+} is shown in the inset.

light and heavy chains is presented in Table I. The ETD mass spectrum obtained from 360 scans with simultaneous fragmentation of three different IgG precursor ions (charge states 53+, 54+, and 55+) shows 46 *c*-ions, 31 $z^{\bullet}$-ions, and 23 *y*-ions for the light chain, corresponding to 72 unique backbone cleavages, and 48 *c*-ions, 35 $z^{\bullet}$-ions, and 21 *y*-ions, equivalent to 90 unique backbone cleavages, for the heavy chain (Fig. 5, *black bars*). In the heavy chain, the Glu^1 residue was observed to be also in pyroglutamic acid (pyroGlu) form, as highlighted in purple in Fig. 5. The total number of 162 identified unique backbone cleavages obtained *via* ETD of the three charge states of IgG precursor ions, taking into account the 214 residues of the light and 451 residues of the heavy chain (altogether resulting in 663 potential backbone cleavage sites), corresponds to 24.4% sequence coverage. Note the cleavages at both sides of proline residues (whose N–C_α bond cleavage in ETD would not result in separated product ions). Furthermore, although most of the assigned cleavage sites are located in the disulfide-bond-free regions, 22 backbone

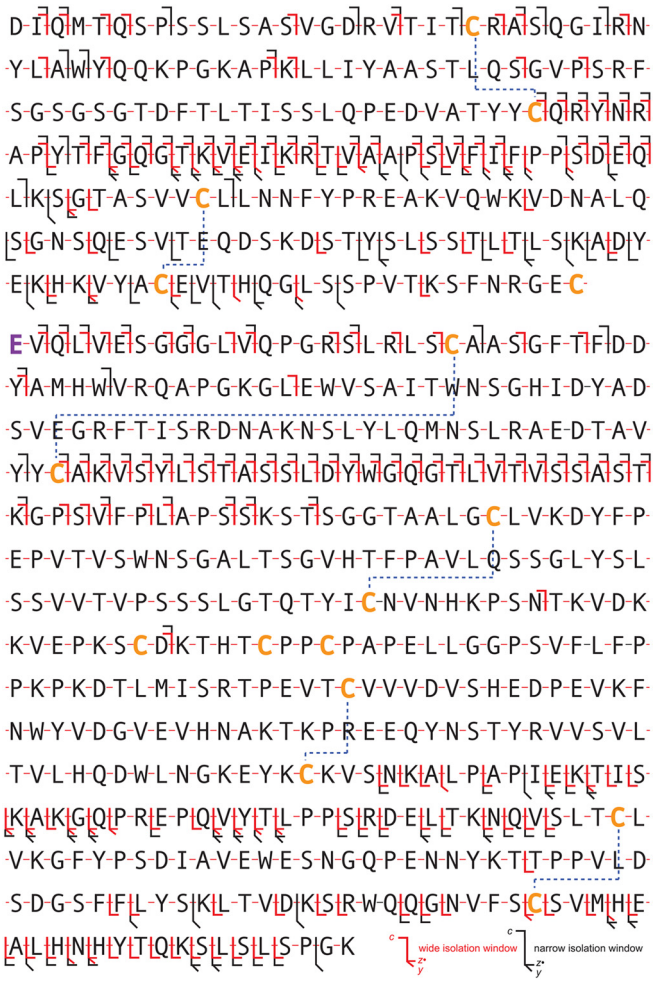

FIG. 5. **Fragmentation map of light (*top*) and heavy (*bottom*) chains of Humira IgG.** Cleavage sites identified for experiments conducted with isolation windows of 100 *m/z* (narrow window, centered at 2750 *m/z*) or 600 *m/z* (wide window, centered at 2900 *m/z*) are indicated in *black* and *red*, respectively. Cysteine residues are represented in *orange*, and intermolecular disulfide bonds are indicated by the *blue dashed lines*. On the heavy chain, the detected pyroGlu[1] mutation is highlighted in *purple*.

cleavages for the light chain and 10 for the heavy chain are notably located in disulfide-protected portions of the polypeptide sequence. Finally, it is noteworthy that the central portion of the light chain, comprising parts of both variable and constant domains, has been extensively sequenced, with most of the backbone cleavages confirmed by the identification of fragments containing information about the N terminus (*c*-ions) and the C terminus ($z^{\bullet}$- and/or *y*-ions). However, the central portion of the heavy chain (including the glycosylation site) was not sequenced at all.

ETD-based Top-down MS: Wide Isolation Window—The wider ion isolation window (600 *m/z* units, including precursor ions from 47+ to 57+ charge states), which might open new dissociation channels, was employed in order to further improve the ETD sequence coverage. Indeed, ETD of precursor

TABLE I
Summary of identified product ions from top-down MS of IgGs

	Light chain				Heavy chain				Total sequence coverage
	N-Term. product ions	C-Term. product ions	Number of unique cleavages	Chain sequence coverage	N-Term. product ions	C-Term. product ions	Number of unique cleavages	Chain sequence coverage	
Orbitrap MS ETD, 360 scans, narrow isolation window[a]	46	54	72	33.8%	48	56	90	20%	24.4%
Orbitrap MS ETD, 1000 scans, wide isolation window[a]	45	43	63	29.6%	57	71	117	26%	27.1%
Orbitrap MS ETD, combined[b]	54	67	92	43.2%	60	85	125	27.8%	**32.7%**
qTOF MS ETD[c]	21	15	31	14.4%	11	62	73	16.1%	15.4%
Orbitrap MS CID[d]	24	32	53	24.8%	26	20	42	9.5%	14.5%

[a] Measurements performed in the present study on intact human IgG1, *kappa*, with *c*-ions considered for the N-terminus and $z^{\bullet}$- and *y*-ions considered for the C-terminus.
[b] Values calculated by combining the backbone cleavage sites of the two Orbitrap FTMS experiments.
[c] Measurements performed in a previous work (Ref. 25) on an intact IgG1, *kappa*, with *c*-ions considered for the N-terminus and $z^{\bullet}$-ions considered for the C-terminus.
[d] Data derived from Ref. (29); measurements performed on reduced and alkylated human IgG2, with *b*-ions considered for the N-terminus and *y*-ions considered for the C-terminus.

ions from the wide isolation window generated 63 and 117 unique backbone cleavages from the light and heavy chains, respectively (Fig. 5, *red bars*). The total number of thus-obtained unique cleavage sites (180) corresponds to 27.1% sequence coverage. Relative to the ETD results obtained with the narrow isolation window, the C-terminal portion of the light chain presents a lower number of assigned backbone cleavages, whereas the sequence coverage of the region between the second and third constant domains (C_H2 and C_H3) and the C-terminal part of the heavy chain is substantially improved. The outlined difference in fragmentation patterns is apparent in the branching ratios of product ions formed. Indeed, the total number of product ions containing information on the C terminus, namely, $z^\bullet$- and *y*-type ions, was 56 in ETD with the narrow isolation window, whereas it reached 71 for ETD with the wide isolation window for the heavy chain (Table I). Conversely, for the light chain, the same number decreased from 54 for the former to 43 for the latter ion selection conditions. Considering the good SNR characterizing both analyzed mass spectra, the observed differences in sequence coverage at the C terminus are most likely due to the use of different ETD precursor ions for the two experimental sequences.

To adequately evaluate the progress made by employing Orbitrap ETD MS/MS for the structural analysis of intact and S–S bond reduced IgG, a comparison with previous work employing ETD MS/MS on a qTOF MS (see Scheme 2 in Ref. (25)) and CID MS/MS on an Orbitrap FTMS (29) can be done (Table I). Note that CID experiments were performed on reduced and alkylated IgG of a different subclass (IgG2, not IgG1). For ETD experiments, the analyzed human IgGs were different only in the variable domains, as they belonged to the same subclass and had the same *kappa*-type light chain. An appreciable increase in sequence coverage provided by ETD on Orbitrap FTMS is apparent (Table I). After we combined the results of narrow and wide isolation window ETD Orbitrap FTMS experiments, the final number of unique backbone cleavage sites rose to 217, representing 32.7% sequence coverage. A detailed investigation of the dependence of sequence coverage on the number of scans has yet to be addressed.

DISCUSSION

Given their multimeric structure comprising two heavy and two light chains, complex intra- and intermolecular disulfide connectivity, and heterogeneous glycosylation on heavy chains and their high molecular weight (~150 kDa), the full characterization of intact IgGs represents a difficult challenge for any MS platform. The state-of-the-art high resolution Orbitrap FTMS allows LC-timescale-compatible intact IgG ionization, charge state selection in a range up to 4000 *m/z*, and fragmentation by both slow-heating methods (*e.g.*, CID and higher energy collisional dissociation) and radical chemistry-based dissociation (*e.g.*, ETD). It also supports the detection of isotopically resolved, multiply charged product ions present in a complex mixture, enabling a top-down MS approach for the structural analysis of intact IgGs. Here, we have demonstrated that time-domain transient signal averaging from a number of consecutive LC-MS/MS experiments before FT signal processing and peak picking significantly improves the performance of Orbitrap FTMS-based top-down MS. We note that although state-of-the-art top-down proteomics of 10 to 50 kDa proteins is already performed with on-line nanoLCMS, the analysis of intact proteins heavier than 50 kDa is often performed after off-line LC-based protein purification followed by off-line nanospray-MS. We opted for an on-line LC-MS/MS approach here because it is more universal than the off-line approach in terms of the types of samples to be addressed, as well as its suitability for automated quality control workflows. Indeed, the near-future goal of the top-down proteomics is to perform analyses of complex protein mixtures that contain heavy proteins as large as 150 to 200 kDa. With an increase in MS sensitivity and speed of high resolution data acquisition, substantially fewer LC-MS/MS runs will be required for protein characterization.

In the current work, the observed increase in SNR rose as expected with the square root of the number of scans; specifically, we estimated a roughly 4-fold to 8-fold gain in SNR from a single LC-MS/MS experiment to the final mass spectra. Furthermore, to maximize the number of assigned unique cleavage sites, we not only averaged 1000 scans, but we also used a large (600 *m/z*) precursor ion isolation window. As a result, the data presented here demonstrate a 2-fold higher sequence coverage than was obtained on a similar human IgG1 in a prior ETD implementation for top-down MS analysis of IgGs. In addition, we report the partial cyclization of Glu^1 to $pyroGlu^1$ on the IgG heavy chain. We note that significant structural differences between IgG variants considered in Table I certainly influence ETD MS/MS performance. Further work should be dedicated to comparing similar IgG subclasses. Also, information about the ETD preference for a particular IgG sequence or higher order structure provides an additional source of information on the ETD fundamentals.

The novelty of the results presented here for ETD-based top-down MS is primarily in the substantially improved analytical characteristics of the employed experimental set-up that increase the overall capabilities of the method and allow an important step to be taken toward its routine application. Although previous work demonstrated the proof-of-principle implementation, it also demonstrated the corresponding limitations, specifically in terms of the mass resolving power. The large number of laboratories equipped nowadays with high-resolution Orbitrap FTMS instrumentation suggests a high impact of the results described here. Nevertheless, similar to previously reported results, we were not able to sequence long portions of the constant domains of light chains or the entire central portion of the heavy chain, presumably because of a combination of disulfide-bond networks and the partial

retention of the secondary and tertiary structures of the IgG in the gas phase, which would explain the almost complete sequence coverage obtained for the flexible, unstructured loops connecting consecutive domains in the light and heavy chains (see Fig. 5). We are currently addressing these issues by implementing ion activation before and after ETD reaction, unfolding IgG *via* the partial reduction of disulfide bonds, and increasing the number of protonated sites *via* precursor ion supercharging. Future improvements in instrumentation—for example, the use of a compact high-field Orbitrap mass analyzer or Orbitrap Elite FTMS instrument or improved ion transfer and trapping—are expected to increase substantially the speed of analysis and reduce the number of scans required for top-down analysis.

Acknowledgments—We are grateful to Anton Kozhinov for assistance with the data analysis.

* This work was supported by the Swiss National Science Foundation (SNF Project No. 200021-125147/1), the Joint Russia-Switzerland Research Program (Grant No. 128357), the EU FP7 PROSPECTS network (Grant No. HEALTH-F4-2008-201648), the Chicago Biomedical Consortium, and the National Institutes of Health (GM 067193 and DA 018310).

[S] This article contains supplemental Fig. S1.

‖ To whom correspondence should be addressed: Prof. Yury O. Tsybin, EPFL ISIC LSMB, BCH 4307, 1015 Lausanne, Switzerland, E-mail: yury.tsybin@epfl.ch.

REFERENCES

1. Cui, W., Rohrs, H. W., and Gross, M. L. (2011) Top-down mass spectrometry: recent developments, applications and perspectives. *Analyst* **136,** 3854–3864
2. Kellie, J. F., Tran, J. C., Lee, J. E., Ahlf, D. R., Thomas, H. M., Ntai, I., Catherman, A. D., Durbin, K. R., Zamdborg, L., Vellaichamy, A., Thomas, P. M., and Kelleher, N. L. (2010) The emerging process of top down mass spectrometry for protein analysis: biomarkers, protein-therapeutics, and achieving high throughput. *Mol. Biosyst.* **6,** 1532–1539
3. Tipton, J. D., Tran, J. C., Catherman, A. D., Ahlf, D. R., Durbin, K. R., and Kelleher, N. L. (2011) Analysis of intact protein isoforms by mass spectrometry. *J. Biol. Chem.* **286,** 25451–25458
4. Chamot-Rooke, J., Mikaty, G., Malosse, C., Soyer, M., Dumont, A., Gault, J., Imhaus, A. F., Martin, P., Trellet, M., Clary, G., Chafey, P., Camoin, L., Nilges, M., Nassif, X., and Dumenil, G. (2011) Posttranslational modification of pili upon cell contact triggers N. meningitidis dissemination. *Science* **331,** 778–782
5. Schluter, H., Apweiler, R., Holzhutter, H. G., and Jungblut, P. R. (2009) Finding one's way in proteomics: a protein species nomenclature. *Chem. Cent. J.* **3,** 11
6. Zhang, J., Zhang, H., Ayaz-Guner, S., Chen, Y. C., Dong, X., Xu, Q., and Ge, Y. (2011) Phosphorylation, but not alternative splicing or proteolytic degradation, is conserved in human and mouse cardiac troponin T. *Biochemistry* **50,** 6081–6092
7. Nikolaev, E. N., Boldin, I. A., Jertz, R., and Baykut, G. (2011) Initial experimental characterization of a new ultra-high resolution FTICR cell with dynamic harmonization. *J. Am. Soc. Mass Spectr.* **22,** 1125–1133
8. Tsybin, Y. O., Ramstrom, M., Witt, M., Baykut, G., and Hakansson, P. (2004) Peptide and protein characterization by high-rate electron capture dissociation Fourier transform ion cyclotron resonance mass spectrometry. *J. Mass Spectrom.* **39,** 719–729
9. Patrie, S. M., Ferguson, J. T., Robinson, D. E., Whipple, D., Rother, M., Metcalf, W. W., and Kelleher, N. L. (2006) Top down mass spectrometry of $<$ 60-kDa proteins from Methanosarcina acetivorans using quadrupole FTMS with automated octopole collisionally activated dissociation. *Mol. Cell. Proteomics* **5,** 14–25
10. Compton, P. D., Zamdborg, L., Thomas, P. M., and Kelleher, N. L. (2011) On the scalability and requirements of whole protein mass spectrometry. *Anal. Chem.* **83,** 6868–6874
11. Scigelova, M., Hornshaw, M., Giannakopulos, A., and Makarov, A. (2011) Fourier transform mass spectrometry. *Mol. Cell. Proteomics* **10,** O111.009431
12. Tran, J. C., and Doucette, A. A. (2009) Multiplexed size separation of intact proteins in solution phase for mass spectrometry. *Anal. Chem.* **81,** 6201–6209
13. Ge, Y., Rybakova, I. N., Xu, Q., and Moss, R. L. (2009) Top-down high-resolution mass spectrometry of cardiac myosin binding protein C revealed that truncation alters protein phosphorylation state. *Proc. Natl. Acad. Sci. U.S.A.* **106,** 12658–12663
14. Zubarev, R. A., Kelleher, N. L., and McLafferty, F. W. (1998) Electron capture dissociation of multiply charged protein cations. A nonergodic process. *J. Am. Chem. Soc.* **120,** 3265–3266
15. Zubarev, R. A. (2003) Reactions of polypeptide ions with electrons in the gas phase. *Mass Spectrom. Rev.* **22,** 57–77
16. Syka, J. E. P., Coon, J. J., Schroeder, M. J., Shabanowitz, J., and Hunt, D. F. (2004) Peptide and protein sequence analysis by electron transfer dissociation mass spectrometry. *Proc. Natl. Acad. Sci. U.S.A.* **101,** 9528–9533
17. Mirgorodskaya, E., Roepstorff, P., and Zubarev, R. A. (1999) Localization of O-glycosylation sites in peptides by electron capture dissociation in a Fourier transform mass spectrometer. *Anal. Chem.* **71,** 4431–4436
18. Stensballe, A., Jensen, O. N., Olsen, J. V., Haselmann, K. F., and Zubarev, R. A. (2000) Electron capture dissociation of singly and multiply phosphorylated peptides. *Rapid Commun. Mass Spec.* **14,** 1793–1800
19. Molina, H., Matthiesen, R., Kandasamy, K., and Pandey, A. (2008) Comprehensive comparison of collision induced dissociation and electron transfer dissociation. *Anal. Chem.* **80,** 4825–4835
20. Santos, L. F. A., Eberlin, M. N., and Gozzo, F. C. (2011) IRMPD and ECD fragmentation of intermolecular cross-linked peptides. *J. Mass Spectrom.* **46,** 262–268
21. Zubarev, R. A., Kruger, N. A., Fridriksson, E. K., Lewis, M. A., Horn, D. M., Carpenter, B. K., and McLafferty, F. W. (1999) Electron capture dissociation of gaseous multiply-charged proteins is favored at disulfide bonds and other sites of high hydrogen atom affinity. *J. Am. Chem. Soc.* **121,** 2857–2862
22. Zubarev, R. A., Horn, D. M., Fridriksson, E. K., Kelleher, N. L., Kruger, N. A., Lewis, M. A., Carpenter, B. K., and McLafferty, F. W. (2000) Electron capture dissociation for structural characterization of multiply charged protein cations. *Anal. Chem.* **72,** 563–573
23. Wu, S. L., Jiang, H. T., Hancock, W. S., and Karger, B. L. (2010) Identification of the unpaired cysteine status and complete mapping of the 17 disulfides of recombinant tissue plasminogen activator using LC-MS with electron transfer dissociation/collision induced dissociation. *Anal. Chem.* **82,** 5296–5303
24. Valeja, S. G., Kaiser, N. K., Xian, F., Hendrickson, C. L., Rouse, J. C., and Marshall, A. G. (2011) Unit mass baseline resolution for an intact 148 kDa therapeutic monoclonal antibody by Fourier transform ion cyclotron resonance mass spectrometry. *Anal. Chem.* **83,** 8391–8395
25. Tsybin, Y. O., Fornelli, L., Stoermer, C., Luebeck, M., Parra, J., Nallet, S., Wurm, F. M., and Hartmer, R. (2011) Structural analysis of intact monoclonal antibodies by electron transfer dissociation mass spectrometry. *Anal. Chem.* **83,** 8919–8927
26. Zhang, Z. Q., Pan, H., and Chen, X. Y. (2009) Mass spectrometry for structural characterization of therapeutic antibodies. *Mass Spectrom. Rev.* **28,** 147–176
27. Sheridan, C. (2010) Fresh from the biologic pipeline-2009. *Nat. Biotechnol.* **28,** 307–310
28. Zhang, Z., and Shah, B. (2007) Characterization of variable regions of monoclonal antibodies by top-down mass spectrometry. *Anal. Chem.* **79,** 5723–5729
29. Bondarenko, P. V., Second, T. P., Zabrouskov, V., Makarov, A. A., and Zhang, Z. Q. (2009) Mass measurement and top-down HPLC/MS analysis of intact monoclonal antibodies on a hybrid linear quadrupole ion trap-Orbitrap mass spectrometer. *J. Am. Soc. Mass Spectrom.* **20,** 1415–1424
30. Senko, M. W., Canterbury, J. D., Guan, S., and Marshall, A. G. (1996) A high-performance modular data system for Fourier transform ion cyclo-

tron resonance mass spectrometry. *Rapid Commun. Mass Spectrom.* **10,** 1839–1844
31. Perelman, D. H., Moscovets, E., Shwe, H., and Kyin, S. (2012) Analysis of transient data from an Orbitrap mass spectrometer with filter diagonalization method. *Proceedings of the 60th American Society for Mass Spectrometry (Santa Fe, NM) Conference on Mass Spectrometry and Allied Topics, Vancouver, Canada,* May 20–24, 2012
32. Blakney, G. T., Hendrickson, C. L., and Marshall, A. G. (2011) Predator data station: a fast data acquisition system for advanced FT-ICR MS experiments. *Int. J. Mass Spectrom.* **306,** 246–252
33. Zamdborg, L., LeDuc, R. D., Glowacz, K. J., Kim, Y. B., Viswanathan, V., Spaulding, I. T., Early, B. P., Bluhm, E. J., Babai, S., and Kelleher, N. L. (2007) ProSight PTM 2.0: improved protein identification and characterization for top down mass spectrometry. *Nucleic Acids Res.* **35,** W701–W706
34. Savitski, M. M., Kjeldsen, F., Nielsen, M. L., and Zubarev, R. A. (2007) Hydrogen rearrangement to and from radical z fragments in electron capture dissociation of peptides. *J. Am. Soc. Mass Spectrom.* **18,** 113–120
35. Ledvina, A. R., McAlister, G. C., Gardner, M. W., Smith, S. I., Madsen, J. A., Schwartz, J. C., Stafford, G. C., Jr., Syka, J. E., Brodbelt, J. S., and Coon, J. J. (2009) Infrared photoactivation reduces peptide folding and hydrogen-atom migration following ETD tandem mass spectrometry. *Angew Chem. Int. Ed. Engl.* **48,** 8526–8528
36. Jefferis, R. (2005) Glycosylation of recombinant antibody therapeutics. *Biotechnol. Progr.* **21,** 11–16
37. Kim, W. D., Tokunaga, M., Ozaki, H., Ishibashi, T., Honda, K., Kajiura, H., Fujiyama, K., Asano, R., Kumagai, I., Omasa, T., and Ohtake, H. (2010) Glycosylation pattern of humanized IgG-like bispecific antibody produced by recombinant CHO cells. *Appl. Microbiol. Biot.* **85,** 535–542
38. Nallet, S., Fornelli, L., Schmitt, S., Parra, J., Baldi, L., Tsybin, Y. O., and Wurm, F. M. (2012) Glycan variability on a recombinant IgG antibody transiently produced in HEK-293E cells. *N. Biotechnol.* **29,** 471–476
39. Hansen, R., Dickson, A. J., Goodacre, R., Stephens, G. M., and Sellick, C. A. (2010) Rapid characterization of N-linked glycans from secreted and gel-purified monoclonal antibodies using MALDI-ToF mass spectrometry. *Biotechnol. Bioeng.* **107,** 902–908
40. Tzeng, Y. K., Chang, C. C., Huang, C. N., Wu, C. C., Han, C. C., and Chang, H. C. (2008) Facile MALDI-MS analysis of neutral glycans in NaOH-doped matrixes: microwave-assisted deglycosylation and one-step purification with diamond nanoparticles. *Anal. Chem.* **80,** 6809–6814
41. Ledvina, A. R., Beauchene, N. A., McAlister, G. C., Syka, J. E., Schwartz, J. C., Griep-Raming, J., Westphall, M. S., and Coon, J. J. (2010) Activated-ion electron transfer dissociation improves the ability of electron transfer dissociation to identify peptides in a complex mixture. *Anal. Chem.* **82,** 10068–10074
42. Sterling, H. J., and Williams, E. R. (2009) Origin of supercharging in electrospray ionization of noncovalent complexes from aqueous solution. *J. Am. Soc. Mass Spectrom.* **20,** 1933–1943
43. Valeja, S. G., Tipton, J. D., Emmett, M. R., and Marshall, A. G. (2010) New reagents for enhanced liquid chromatographic separation and charging of intact protein ions for electrospray ionization mass spectrometry. *Anal. Chem.* **82,** 7515–7519
44. Yin, S., and Loo, J. A. (2011) Top-down mass spectrometry of supercharged native protein-ligand complexes. *Int. J. Mass Spectrom.* **300,** 118–122
45. Miladinovic, S. M., Fornelli, L., Piech, K. M., Lu, Y., Girault, H. H., and Tsybin, Y. O. (2012) In-spray supercharging of peptides and proteins in electrospray ionization mass spectrometry. *Anal. Chem.* **84,** 4647–4651
46. Kozhinov, A. N., and Tsybin, Y. O. (2012) Filter diagonalization method-based mass spectrometry for molecular and macromolecular structure analysis. *Anal. Chem.* **84,** 2850–2856